A Statistical Analysis of the Morphology of Storm-Enhanced Density Plumes

Patricia Dzwill[1,2], Ercha Aa[1], Shun-Rong Zhang[1], Philip J. Erickson[1]

[1] MIT Haystack Observatory, [2] New Jersey Institute of Technology

Summary

This study provides a statistical analysis of SED plume morphology over the continental United States (CONUS) to show common characteristics over a set intense storms. The results of this project help to build a general knowledge of SEDs and provide a new way to observe and compare SED plume characteristics within and between events.

Key Points

1. **A comprehensive list of 49 SED events over the continental US was identified for periods of intense geomagnetic storms during 2000–2023.**
2. **A first-time statistical analysis of SEDs demonstrates their geomagnetic dependence, seasonal distribution, and solar cycle variation.**
3. **SEDs demonstrate a sub-corotate feature with respect to the Earth, with westward drifting speeds of 50-400 m/s and a duration of 3-10 hours.**

Background

Storm-Enhanced Densities (SED) are disturbances in the plasma of the midlatitude ionosphere that occur during geomagnetic storms. They result in heightened levels of Total Electron Content (TEC) plume structure that stretches sunward and poleward from local afternoon. SED plumes are repeatable phenomena that are dynamic in aspects like their location and intensity based on many conditions that aren't fully known. SED can impact telecommunication, so it is important to better understand their morphology.

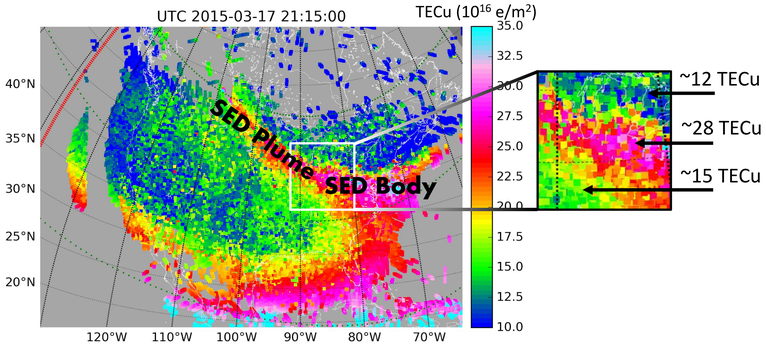

Figure 1: An example of an SED plume from March 17th, 2015 during the largest geomagnetic storm of cycle 24. The SED body and SED plume are labelled. The submap on the right shows the intense plasma density gradient that is characteristic of SED plumes.

Instruments and Databases

GNSS TEC on Madrigal

Global **N**avigation **S**atellite **S**ystem

Vertical TEC data is calculated from GNSS data from 6000+ ground-based receivers and stored in Madrigal, the upper atmosphere database from CEDAR and MIT Haystack.

TEC data is binned by 1° lat × 1° lon × 5 minutes in TECu

TIDAS NmF2

TEC-based **I**onospheric **D**ata **A**ssimilation **S**ystem

3D reconstruction of the full profile of the ionosphere above CONUS assimilated from GNSS TEC, Millstone Hill ISR and other data sources. We utilized the NmF2 (F2 layer peak density) from TIDAS in the results in Figure 4.

Reference:

Aa, E., Dzwill, P., Zhang, S.-R., Erickson, P. J.,(2024). A statistical analysis of the morphology of storm-enhanced density plumes over the north American sector. *Journal of Geophysical Research: Space Physics, 129, e2024JA032750.*

Methodology

Storm Identification

We looked at a list of intense geomagnetic storms (Minimum Sym-H index < -100 nT) and identified 49 storms which exhibited clear SED plumes over CONUS from 2000-2023. For each plume, we recorded the start time, end time, upper latitude bound, and lower latitude bound.

Gaussian Fitting

We fitted a gaussian at each time bin in the interval, over all the SED plume latitudes, then averaged to derive SED plume key features: central longitude (ϕ_0), plume half-width (σ), and plume intensity (h). The variables a, b, and c describe the background TEC value.

$$TEC(\phi) = h \times \exp(-(\phi - \phi_0)^2 / 2\sigma^2) + b + c \times \phi + d \times \phi^2$$

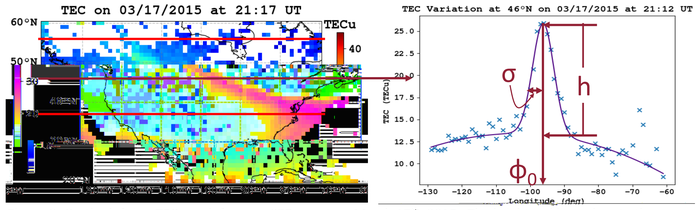

Figure 2: On the left is a TEC graph from an SED event on March 17th, 2015. The bright red lines denote the upper and lower latitude bounds of the SED plume. On the right is the TEC data from 46° latitude from the graph on the left (marked by the dark red arrow) fitted to the gaussian equation at the top. The SED plume key features central longitude (ϕ_0 = -96), plume half-width (σ = 3), and plume intensity (h = 12) are marked with arrows.

Results

The following graphs use the statistical characteristics derived from the gaussian fittings to compare SED features over separate days (Figures 3 and 4) and to geomagnetic activity, time of year, and solar activity (Figures 5 and 6). In Figures 3 and 4, the blue dots represent the mean value during that time over all SED latitudes and the bars represent the standard deviation. In Figures 5 and 6, the dots represent daily mean value of a given characteristic.

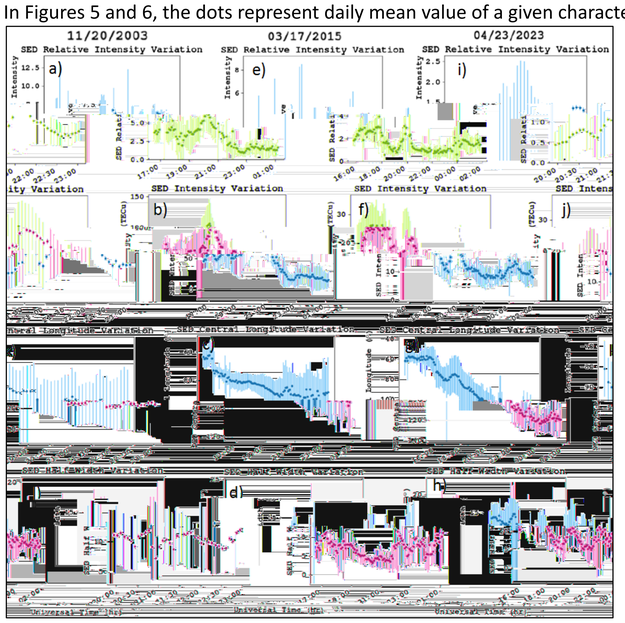

Figure 3: This show the variations over time of key features from the SED events on November 20th, 2003 (a-d), March 17th, 2015 (e-h), and April 23rd, 2023 (i-l). The relative intensity and intensity of the plume (top left and right) tend to peak in the middle of the storm. The SED central longitude (bottom left) tends to move westward over the course of the event. The plume half-width (bottom right) does not tend to increase, decrease, or peak, and instead varies between 5 and 15 degrees.

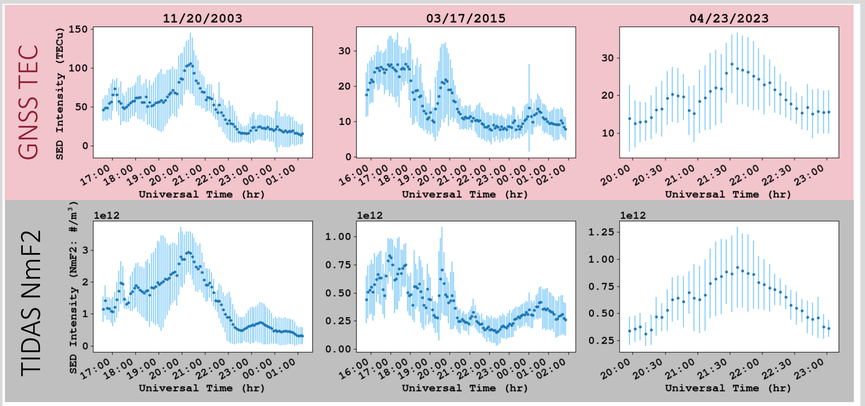

Figure 4: A comparison between SED plume intensity in GNSS TEC data (top) and TIDAS NmF2 data (bottom). This NmF2 data has been characterized with the same method described in Methodology. The TEC data and the NmF2 data display similar variations. They peak around 20:30 UT on 11/20/2003, around 21 UT on 03/17/2015, and around 21:45 UT on 04/23/2023. The deviation over latitude is similar in scale between GNSS TEC values and TIDAS NmF2. This suggests that the plume morphology TEC and NmF2 values vary similarly over latitudes during geomagnetic storms.

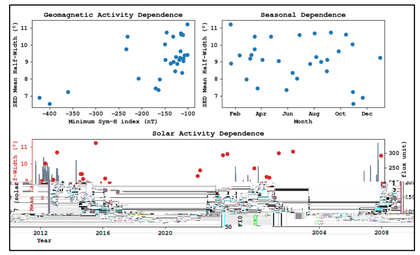

Figure 5: A comparison of SED plume peak log intensity with geomagnetic activity (top left), time of year (top right), and the solar activity (bottom). The top left and bottom graph shows that the 3 SED events with the lowest minimum Sym-H index (which were during the November 2003 superstorm) have a significantly higher SED peak intensity than the other SEDs. This could suggest a correlation between intense geomagnetic/solar activity and SED intensity. Additionally, 5b shows peaks around equinoxes.

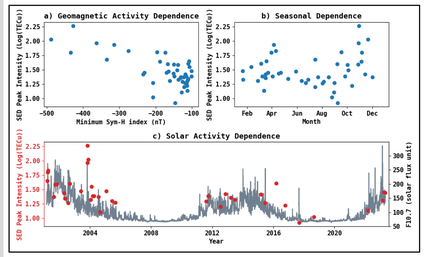

Figure 6: A comparison of SED plume mean half-width with geomagnetic activity, time of year, and the solar activity. Similar to Figure 5, the SED events from the 2003 superstorm stand out due to a noticeably smaller mean half-width in the top left and bottom graphs. This could suggest a correlation between intense geomagnetic/ solar activity and smaller SED plume half-width.

Figure 7: SED statistics by plume duration and horizontal drift speed.

Table 1: Intense Storm list containing the SED over CONUS.

	Storm Date	Sym-H$_{min}$	Sym-H$_{min}$ time	SED start time	SED end time
01	2000-04-06	-320 nT	00:09 UT (+1 day)	19:30 UT	02:05 UT (+1 day)
02	2000-07-15	-347 nT	21:54 UT	22:20 UT	02:30 UT (+1 day)
03	2000-09-17	-203 nT	00:24 UT (+1 day)	23:25 UT	03:05 UT (+1 day)
04	2000-10-04	-141 nT	19:47 UT	17:50 UT	23:30 UT
05	2000-11-06	-176 nT	21:04 UT	17:00 UT	23:15 UT
06	2001-03-19	-109 nT	21:06 UT	19:35 UT	22:45 UT
07	2001-03-31	-437 nT	08:06 UT	17:20 UT	22:30 UT
08	2001-04-11	-280 nT	23:57 UT	18:15 UT	01:10 UT (+1 day)
09	2001-08-17	-131 nT	21:12 UT	19:00 UT	01:20 UT (+1 day)
10	2001-10-02	-188 nT	14:23 UT (+1 day)	19:35 UT	21:50 UT
11	2001-10-28	-150 nT	11:19 UT	18:55 UT	22:55 UT
12	2002-04-18	-151 nT	07:48 UT	18:00 UT	23:10 UT
13	2002-05-11	-110 nT	19:54 UT	19:20 UT	23:30 UT
14	2002-08-02	-115 nT	04:53 UT	19:05 UT	00:30 UT (+1 day)
15	2002-09-07	-168 nT	23:57 UT	19:30 UT	22:50 UT
16	2003-05-29	-166 nT	07:58 UT (+1 day)	19:20 UT	02:55 UT (+1 day)
17	2003-10-29	-391 nT	01:48 UT (+1 day)	19:35 UT	01:20 UT (+1 day)
18	2003-10-30	-432 nT	22:55 UT	20:45 UT	02:15 UT (+1 day)
19	2003-11-20	-490 nT	18:17 UT	16:40 UT	01:15 UT (+1 day)
20	2004-01-22	-137 nT	13:25 UT	17:00 UT	22:30 UT
21	2004-02-11	-107 nT	17:10 UT	17:15 UT	21:35 UT
22	2004-03-09	-101 nT	05:30 UT (+1 day)	17:45 UT	01:15 UT (+1 day)
23	2004-04-03	-149 nT	00:42 UT (+1 day)	20:00 UT	01:30 UT (+1 day)
24	2004-07-22	-123 nT	02:40 UT (+1 day)	21:00 UT	02:30 UT (+1 day)
25	2004-08-30	-128 nT	22:47 UT	19:30 UT	01:30 UT (+1 day)
26	2005-01-21	-101 nT	06:04 UT (+1 day)	22:30 UT	01:00 UT (+1 day)
27	2005-06-12	-112 nT	00:38 UT (+1 day)	19:30 UT	01:00 UT (+1 day)
28	2005-08-31	-119 nT	19:08 UT (+1 day)	17:50 UT	21:30 UT
29	2011-08-05	-126 nT	03:22 UT (+1 day)	20:30 UT	02:40 UT
30	2011-09-26	-116 nT	21:19 UT	20:20 UT	23:50 UT
31	2011-10-24	-160 nT	01:15 UT (+1 day)	23:30 UT	08:25 UT
32	2012-04-23	-125 nT	03:26 UT (+1 day)	18:10 UT	01:00 UT
33	2012-07-15	-123 nT	10:04 UT	18:00 UT	03:45 UT (+1 day)
34	2012-11-13	-118 nT	07:27 UT (+1 day)	20:50 UT	01:30 UT (+1 day)
35	2013-03-17	-132 nT	20:28 UT	17:00 UT	23:50 UT
36	2013-06-28	-111 nT	06:34 UT (+1 day)	18:50 UT	02:30 UT (+1 day)
37	2015-03-17	-234 nT	22:47 UT	15:50 UT	01:50 UT (+1 day)
38	2015-06-22	-208 nT	04:24 UT (+1 day)	19:10 UT	22:00 UT
39	2015-12-21	-117 nT	01:07 UT (+1 day)	16:00 UT	20:45 UT
40	2016-03-06	-110 nT	21:20 UT	20:30 UT	00:50 UT (+1 day)
41	2016-10-13	-114 nT	23:45 UT	15:10 UT	22:10 UT
42	2017-09-07	-146 nT	01:08 UT (+1 day)	23:00 UT	01:30 UT (+1 day)
43	2018-08-25	-206 nT	07:11 UT (+1 day)	23:00 UT	03:00 UT (+1 day)
44	2022-03-13	-113 nT	23:58 UT	23:00 UT	01:40 UT (+1 day)
45	2023-02-27	-161 nT	12:12 UT	18:40 UT	23:50 UT
46	2023-03-23	-169 nT	02:40 UT (+1 day)	20:00 UT	00:30 UT (+1 day)
47	2023-04-23	-233 nT	04:03 UT (+1 day)	20:00 UT	23:00 UT
48	2023-11-05	-189 nT	16:54 UT	17:10 UT	23:50 UT
49	2023-12-01	-132 nT	12:37 UT	16:40 UT	00:40 UT (+1 day)

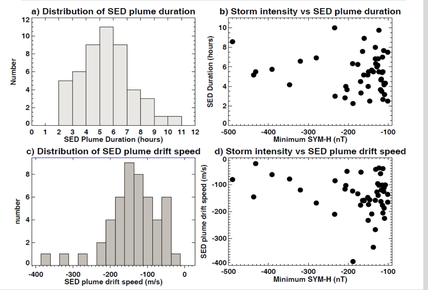

Acknowledgments

We acknowledge and thank NSF for the support to make the 2023 MIT Haystack REU possible and for the awards AGS-1952737 and AGS-2033787.